Desalination and Water Treatment
www.deswater.com

37 (2012) 46–54
January

doi: 10/5004/dwt.2012.2211

Taylor & Francis
Taylor & Francis Group

Study of congo red adsorption onto chitosan coated magnetic iron oxide in batch mode

Huimin Zhu, Manman Zhang, Yaoqiang Liu, Lijuan Zhang, Runping Han*

Department of Chemistry, Zhengzhou University, 100# Kexue Road, Zhengzhou 450001, P.R. China
Tel. +86 371 67781757; Fax: +86 371 67781556; email: rphan67@zzu.edu.cn

Received 7 August 2010; Accepted 21 June 2011

ABSTRACT

The adsorption behavior of congo red (CR) on a magnetic composite (chitosan coated magnetic Fe_3O_4 particle) was studied as a function of initial solution pH, salt concentration, contact time, initial concentration of CR in batch mode. Change of solution pH, adsorption isotherms and their thermodynamic parameters (ΔG^0, ΔH^0, ΔS^0) were discussed. There was little effect of initial pH and salt concentration. The experimental data were fitted to Langmuir, Freundlich, Temkin, Koble–Corrigan and Toth isotherm models. It was found that the Langmuir, Koble–Corrigan and Toth models provided good correlation. The adsorption capacity of CR was obtained from the Langmuir model and found to be 42.62, 55.68, 56.66 mg/g^{-1} at 295, 305, 315 K, respectively. The thermodynamic parameters indicated spontaneous and endothermic process. It was concluded that the adsorption process was main chemical adsorption and the dye-loaded adsorbent can be reused by regeneration with dilute NaOH solution.

Keywords: Congo red; Chitosan coated magnetic iron oxide; Isotherm; Thermodynamic parameters; Adsorption; Regeneration

1. Introduction

Chitosan is obtained from deacetylation of the naturally occurring biopolymer chitin which is the second most abundant polysaccharide in the world after cellulose [1]. So chitosan is a natural, biodegradable, biocompatible and mucoadhesive polymer with permeability enhancement properties. Chitosan can be used for antimicrobial activity, flocculant, coagulant, medicine and cosmetics [2]. Furthermore, this natural polymer possesses several intrinsic characteristics and can be used as an effective adsorbent for the removal of color and heavy metal ions [3,4]. There are two important advantages of chitosan as adsorbent: firstly, its low cost compared to commercial activated carbon; secondly, its outstanding chelation behavior [1].

In order to overcome the difficulties associated with its softness and tendency to agglomerate or form a gel in aqueous solutions, modifications are carried out by coating chitosan on alumina for the removal of Cr(VI) and as on perlite for the removal of Cu(II), on PVC for the removal of Cu(II) and Ni(II), on sand for removal of Cu(II), on bentoite for the removal of reactive dye and on clay for the removal of tannic acid, humic acid, and dyes [5–11]. The composites improve the mechanical strength and specific gravity compared to chitosan. But the composite of chitosan directly coated on magnetic Fe_3O_4 particle is seldom studied.

Wastewaters containing dyes are very difficult to treat, since the dyes are recalcitrant molecules, resistant to aerobic digestion. Another difficulty is treatment of wastewaters containing low concentrations of dye molecules [12]. The presence of very small amounts of dyes in water is highly visible and undesirable. So it is essential to remove color from solution. It is known that adsorption using low-cost adsorbents is an effective and economic method for water decontamination.

*Corresponding author.

Many non-conventional adsorbent materials have been proposed and studied for their ability to remove dyes [13–27]. Congo red (CR, CI 22120, molecule weight 696.68 g mol^{-1}) contains NH_2 and SO_3 functional groups and is an anionic disazo direct dye. It can be metabolized to benzidine, a known human carcinogen. Exposure to the dye has been known to cause an allergic reaction.

In this paper, a composite, chitosan coated on magnetic Fe_3O_4 particle (CCIO), is prepared and used as adsorbent for the removal of CR from solution. The effect of pH, salt concentration and CR concentration on adsorption is studied. The adsorption isotherms and thermodynamics constants are also presented.

2. Materials and methods

2.1. Materials

Chemicals of medium molecular weight chitosan, magnetic Fe_3O_4, oxalic acid, and NaOH were all analytical grade and CR was chemical grade. All chemicals were obtained from the Luoyang Chemical Corporation in China.

The stock solutions of CR (500 mg l^{-1}) were prepared in distilled water. All working solutions were prepared by diluting the stock solution with distilled water to the needed concentrations.

2.2. Preparation of chitosan coated magnetic Fe_3O_4 particle (CCIO)

10.0 g of chitosan was precisely weighed and was slowly added to 250 ml oxalic acid (5 % V:V) solution with continuous stirring for about 4 h to facilitate the formation of viscous gel [7,8]. Then 100 g of magnetic Fe_3O_4 was slowly added to the diluted chitosan gel, stirred for 5 h and was allowed to stay over night. The particles coated with chitosan were neutralized by 0.1 mol l^{-1} NaOH solution to pH 8–9. Then it was washed several times by distilled water. The CCIO was desiccated by microwave irradiation and was grounded.

2.3. Adsorption experiments

Batch experimental studies were carried out with 0.04 g of adsorbent and 10 ml of CR solution of desired concentration in 50 ml flasks except the experiment carried out for testing the effect of dosage on adsorption. The flasks were agitated on a mechanical shaker at 100 rpm for 10 h at a predetermined temperature. In order to study the effect of pH on the adsorption capacity, the initial pH of the solutions was adjusted to a desired value by adding either 0.1 mol l^{-1} H_2SO_4 or 0.1 mol l^{-1} NaOH at 295 K. The pH of the solution (initial pH 7.3) in each flask was not adjusted during other adsorption process. After adsorption, the adsorbent was separated by magnetic separation and the dye concentration in solution was measured.

The concentration of CR in the solution was analyzed using a UV/Vis-3000 spectrophotometer (Shimadzu Brand UV-3000) by monitoring the absorbance changes at a wavelength of maximum absorbance (500 nm).

The data obtained in batch mode studies were used to calculate the adsorbed CR. It was calculated for each sample by using the following expression:

$$q_e = \frac{V(c_0 - c_e)}{m} \quad (1)$$

where q_e is the equilibrium uptake value in mg g^{-1}; V is the sample volume in l; c_0 is the initial CR concentration in mg l^{-1}; c_e is the equilibrium CR concentration in mg l^{-1}; and m is the weight of adsorbent in g.

The percent efficiency of CR removal is calculated as following:

$$p = \frac{c_0 - c_e}{c_0} \times 100\% \quad (2)$$

2.4. Regeneration of dye-loaded adsorbent

The adsorbent (0.04 g) used for the adsorption of 10 ml of 100 mg l^{-1} dye solution was separated from the dye solution and the removal efficiency was calculated. The dye-loaded adsorbent was washed gently to remove any unadsorbed dye with water. Then the dye-loaded adsorbent was agitated with 10 ml of 0.01 mol l^{-1} NaOH solution or 10 ml H_2O (pH 6.0, common solvent) for 30 min and separated. NaOH (OH^-) was used to exchange the adsorbed CR or change the surface property of CCIO and then some adsorbed CR was back to solution while H_2O was used to elute adsorbed CR by weak action. The adsorbent was again washed gently with water and reused as adsorbent to mix with 10 ml of 100 mg l^{-1} dye solution. The removal efficiency was then measured.

2.5. Adsorption isotherms

To optimize the design of an adsorption system for the removal of adsorbate, it is important to establish the most appropriate correlation for the equilibrium data. Various isotherm equations have been used to describe the isotherm curve. Five adsorption isotherm model, Langmuir, Freundlich, Temkin, Koble–Corrigan and Toth models were selected and the nonlinear equations were listed as following.

2.5.1. Langmuir isotherm

The Langmuir adsorption isotherm has been successfully applied to many pollutants adsorption processes and has been the most widely used sorption isotherm for

the sorption of a solute from a liquid solution [28]. The saturated monolayer isotherm can be represented as

$$q_e = \frac{q_m K_L c_e}{1 + K_L c_e} \quad (3)$$

where c_e is the equilibrium concentration(mg l^{-1}); q_e is the amount of CR adsorbed onto per unit mass of CCIO (mg g^{-1}); q_m is q_e for a complete monolayer (mg g^{-1}), a constant related to sorption capacity; and K_L is a constant related to the affinity of the binding sites and energy of adsorption (l mg^{-1}).

2.5.2. Freundlich isotherm

Freundlich isotherm is an empirical equation describing adsorption onto a heterogeneous surface. The Freundlich isotherm is commonly presented as

$$q_e = K_F c_e^{1/n_F} \quad (4)$$

where K_F and n are the Freundlich constants related to the adsorption capacity and adsorption intensity of the adsorbent, respectively [29].

2.5.3. Temkin isotherm

The derivation of the Temkin isotherm assumes that the fall in the heat of adsorption is linear rather than logarithmic, as implied in the Freundlich equation. The Temkin isotherm is as following

$$q_e = A + B\ln c_e \quad (5)$$

where A and B are isotherm constants [30].

2.5.4. Koble–Corrigan isotherm

Koble–Corrigan model is three-parameter equation for the representing equilibrium adsorption data. It is a combination of the Langmuir and Freundlich isotherm type models and is given by Eq. (6):

$$q_e = \frac{A c_e^n}{1 + B c_e^n} \quad (6)$$

where A, B and n are the Koble–Corrigan parameters [31].

2.5.5. Toth isotherm

Toth model is another three-parameter equation for the representing equilibrium adsorption data [32]. Toth model is given as Eq. (7)

$$q_e = \frac{q_m c_e}{[K_{Th} + c_e^t]^{1/t}} \quad (7)$$

where q_m is the maximum uptake (mg g^{-1}), K_{Th} is the Toth model constant and t is the Toth model exponent.

The relative parameters of each equation are obtained using least square sum (SS) between the calculated data and experimental data by nonlinear regressive analysis. The calculated expression of SS is as following:

$$SS = \sum (q_c - q_e)^2 \quad (8)$$

where q_c is the predicted (calculated) quantity of CR adsorbed onto CCIO according to adsorption models and q_e is the experimental data.

3. Results and discussion

3.1. Effect of CCIO dosage

The effect of CCIO dosage on adsorption of CR is shown in Fig. 1.

From Fig. 1, it followed the usual pattern of increasing removal efficiency as the adsorbent dosage increased. This corresponded to an increase in active sites for adsorption, but the value of q_e decreased. At higher adsorbent dosage, there is a very fast superficial adsorption onto the adsorbent surface that produces a lower solute concentration in the solution than when adsorbent dose is lower. Thus with increasing adsorbent dose, the amount of CR adsorbed per unit mass of CCIO reduced, causing a decrease in q_e value. The decrease in amount of dye adsorbed q_e with increasing adsorbent mass is due to the split in the concentration gradient between dye concentration in the solution and the dye concentration in the surface of the adsorbent. Other researches had similar results [15,21]. So the dose of 0.04 g was chosen in present study.

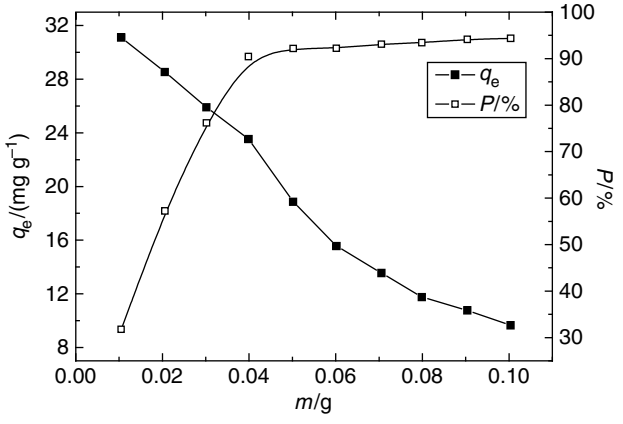

Fig. 1. The effect of CCIO dosage on adsorption and percent removal efficiency (c_0 = 100 mg l^{-1}).

3.2. Effect of pH on adsorption

It is well known that the pH of the system is an important variable in the adsorption process. The charge of the adsorbate and the adsorbent often depends on the pH of the solution [1,13]. Fig. 2 shows the variation of CR adsorption on CCIO at different solution pH and the change of pH value.

From Fig. 2, the effect of initial pH (2–11) was not significant. So the pH of CR solution (near 7.3) was not adjusted in the next experiments. Fig. 1 also showed the difference between initial and equilibrium pH of dye solution. The value of equilibrium pH increased when the initial pH was lower than 7, while the value of equilibrium pH decreased when the initial pH was higher than 7. In another words, some hydrogen ions were consumed during adsorption process at pH<7 while some hydrogen ions were released at pH>7. The effect of pH on dye adsorption was different due to experimental condition, dye structure, ion strength and was particularly discussed by Grini & Badot [1].

In order to understand the role of pH on the adsorption process, the surface charge of adsorbent particles was determined by measuring zeta potential. Surface charge of adsorbent was positive in acidic pH, which decreases gradually with increase in pH and pass through zero potential at pH 6.8. The explanation for pH change was that under acidic conditions hydrogen atoms (H^+) in the solution could protonate the amine groups ($–NH_2$) of chitosan and thus cause the increase in pH [1]:

$$R'\text{-}NH_2 + H^+ \rightleftharpoons R'\text{-}NH_3^+$$

As solution pH was over 7, the final pH decreased. The phenomena may be explained by the accessibility of hydroxyl groups in chitosan. The deprotanation of the hydroxyl group occurred under caustic conditions [33]:

$$CH_2OH + OH^- \rightleftharpoons CH_2O^- + H_2O$$

At pH higher, the excessive hydroxyl ions may compete with the dye anions and hence a slow reduction in dye uptake was observed. However, significant adsorption of the anionic dye on the adsorbent still occurred at alkaline pH values. This suggests that the chemisorption mechanism might be operative [34].

3.3. Effect of contact time on adsorption

Effect of contact time on adsorption is important. Fig. 3 illustrates the effect of contact time on CR adsorption.

It was observed from Fig. 3 that the adsorption rates were initially rapid due to the readily accessible sites that subsequently became much slower. The results showed that kinetics of adsorption of CR consisted of two phases: an initial rapid phase where adsorption was fast and contributed significant to equilibrium uptake and a slower second phase whose contribution to the total CR adsorption was relatively small. The first phase was the instantaneous adsorption stage or external surface adsorption. The second phase was the gradual adsorption stage and finally the CR uptake reached equilibrium. So the adsorption of CR onto CCIO may be controlled by external mass transfer followed by intra particle diffusion mass transfer [34,35]. Similar results were obtained from other research [15,22].The contact (agitation) time was fixed at 600 min for the rest of the batch experiments to make sure that equilibrium was reached.

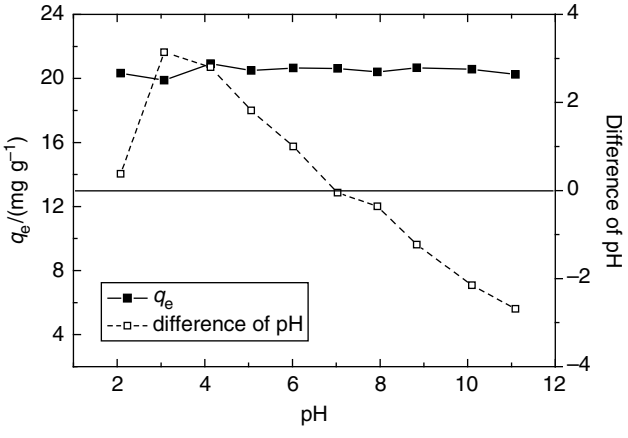

Fig. 2. Effect of initial solution pH on CR adsorption and the difference of pH before and after adsorption (T = 295 K, c_0 = 100 mg l^{-1}).

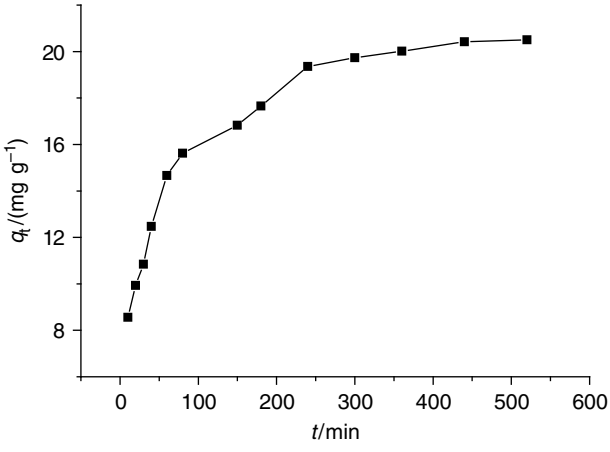

Fig. 3. Effect of contact time on adsorption (T = 295 K, c_0 = 100 mg l^{-1}).

3.4. Effect of salt concentration

In typical dyeing systems it is well known that certain additives such as salts and surfactants can either accelerate or retard dye adsorption processes. Fig. 4 shows the effect of various concentration of NaCl and Na_2SO_4 solution on adsorption.

It was observed from Fig. 4 that the effect of salt concentration was not significant. There was also no significant difference of adsorption quantity when NaCl or Na_2SO_4 existed in solution. About cationic dye adsorption on adsorbent, existence of salt was disadvantage of adsorption [15]. But for anionic dye adsorption, existence of salt was favor of adsorption [16]. Al-Degs et al. studied ionic strength on reactive dye adsorption by activated carbon and found that the removal of dye increased with increase in the ionic strength of solution due to aggregation of reactive dyes in solution [36]. Maurya et al. studied the effect of ionic strength on methylene blue and rhodamine B adsorption by dead macro fungi and found that an increase in ionic strength exhibited an adverse effect on dye adsorption capacity and the extent of pH and ionic strength effect was related to dye structure [37]. In this study, the result was different.

The reason of salt effect is mainly due to the difference of adsorbent and structure of dyes. Salts may screen the electrostatic interaction of opposite charges or decrease the repulsion of positive or negative charge ions in adsorbents and the dye molecules and enhance adsorption capacity. Another reason may be that competitive adsorption exists between salt ions and dye ions with the same charge and this decreases adsorption capacity. Third reason is that the activity of CR and the active sites decrease with the increase in ionic strength. So the extent of adsorption may be affected. The experimental results also showed that ion-exchange mechanism may not be the major adsorption mechanism as there was a little effect of pH and salt on adsorption.

3.5. Effect of initial dye concentration

The effect of the initial concentration of CR on the values of q_e is shown in Fig. 5.

It was shown from Fig. 5 that equilibrium uptake increased with the increasing of initial CR concentrations at the range of experimental concentration. This was a result of the increase in the driving force (the concentration gradient) with an increase in the initial CR concentrations. In the same conditions, if the concentration of CR in solution was higher, the active sites of adsorbent were surrounded by more CR ions, and thus enhanced adsorption. The results also suggested the presence of hydrophobic interactions between dye molecules and dye-materials [1]. Furthermore, dye aggregation may also occur on the adsorbate surface at high dye concentration.

Higher adsorptive capacity of CR was also observed in higher temperature, especially the effect of temperature was manifest for high initial dye concentration. So it evidently affected the mass transfer resistance. Temperature affected not only the chemical potential of the material but also the solubility of the dye molecules. This was due to the increasing tendency of adsorbate ions to adsorb from the solution to the interface with increase in solution temperature [1]. The increase of the equilibrium adsorption with increase in temperature indicated that the adsorption of CR ions onto CCIO was endothermic in nature. This result could indicate a physicochemical adsorption.

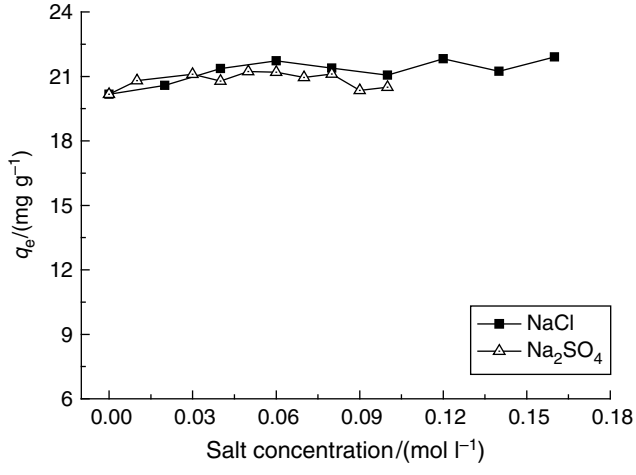

Fig. 4. Effect of salt concentration on adsorption (c_0 = 100 mg l^{-1}).

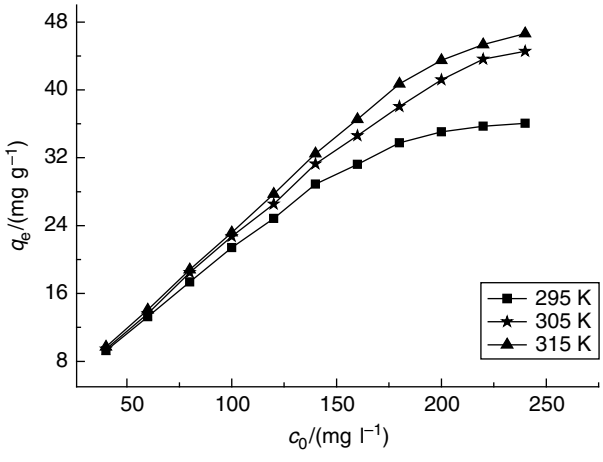

Fig. 5. The effect of initial CR concentration on adsorption at different temperature.

3.6. Determination of adsorption isotherm parameters

The analysis requires equilibrium to better understand the adsorption process. In this paper, the Langmuir, Freundlich, Temkin, Koble–Corrigan and Toth models were applied. An adsorption isotherm is characterized by certain constants which values express the surface properties and affinity of the adsorbent. It can also be used to find the adsorption capacity of adsorbent.

All relative parameters of isotherm equations, determination coefficients (R^2) and values of *SS* are listed in Table 1, respectively. Fig. 6 shows the experimental equilibrium curve and fitted equilibrium curves by five selected isotherms, respectively.

From Table 1, it was observed that values of R^2 from Toth, Langmuir and Koble–Corrigan models were higher than those from Temkin and Freundlich models, while the values of *SS* from former three models were smaller. This showed that the Toth, Langmuir and Koble–Corrigan models were better used to fit the experimental equilibrium data. The lowest determination coefficient with largest value of *SS* for the Freundlich isotherm confirmed the nonapplicability of this model for CR/CCIO systems. Comparison between the experimental data and fitted curves in Fig. 6, the Toth, Langmuir and Koble–Corrigan isotherms can predict equilibrium adsorption behavior and Toth and Langmuir isotherms were better as there were higher value of R^2 and lower value of *SS* in Table 1.

Langmuir and Toth constant, q_m, represents the monolayer saturation at equilibrium. The values of q_m obtained from the Langmuir model were 42.62, 55.68, 56.66 mg g^{-1} at 295, 305, 315 K, respectively. From Table 1, value of q_m from Langmuir model was bigger than that from Toth model. This implied that the predicted value about same parameter from different models be different.

From Table 1 and Fig. 6, Langmuir isotherm predicted the monolayer coverage of CR on CCIO particles. For Toth isotherm, the parameter *t* was away from unity and this result showed that the some heterogeneous was the system. So it was concluded that the adsorption process may be complex.

The composite of CCIO, had larger quantity of CR adsorption than Fe_3O_4 particles (data not shown). Chatterjee et al. collected the values of q_m about other adsorbents for CR adsorption, such as chitosan hydrobeads (92.59 mg g^{-1}), waste wollestonite (1.21 mg g^{-1}), biogas waste slurry (9.5 mg g^{-1}), paddy straw (1.01 mg g^{-1}),waste banana pith (20.29 mg g^{-1}, Fe (III)/Cr (III) (44.0 mg g^{-1}), waste orange peal, Neem leaf powder (41.2 mg g^{-1}), waste red mud (4.05 mg g^{-1}), *Aspergillus niger* biomass (14.16 mg g^{-1}), activated carbon prepared from coir pith (6.7 mg g^{-1}), granulated (13.80 mg g^{-1}) and powdered activated carbon (16.81 mg g^{-1}) [38]. So the capacity of CCIO for CR removal is higher. Furthermore, the adsorbent separation from solution was easy by magnetic method. Consequently, CCIO was suitable as an adsorbent for removal or immobilization of CR from aqueous solution.

Table 1
Isotherm constants for CR adsorption at different temperatures

Isotherm constants	Temperature/K		
	295	305	315
Langmuir			
K_L (l mg^{-1})	0.0727±0.0064	0.0753±0.0072	0.114±0.016
q_m (mg g^{-1})	42.62±1.14	55.68±1.97	56.66±2.79
R^2	0.987	0.986	0.969
SS	1.35	2.25	5.89
Freundlich			
K_F	8.50±1.25	9.07±1.21	12.29±1.81
$1/n_F$	0.339±0.038	0.410±0.039	0.364±0.047
R^2	0.921	0.943	0.897
SS	7.98	9.78	19.3
Temkin			
A	–1.62±1.75	–2.75±1.90	4.13±2.57
B	8.79±0.53	11.92±0.66	11.33±0.10
R^2	0.968	0.972	0.935
SS	3.23	4.51	12.23
Koble–Corrigan			
A	2.82±0.76	4.00±0.10	4.85±1.68
B	0.0674±0.0154	0.0730±0.0139	0.0918±0.0273
N	1.04±0.12	1.03±0.13	1.17±0.20
R^2	0.987	0.986	0.917
SS	1.49	2.52	6.10
Toth			
q_m (mg g^{-1})	40.13±2.46	52.80±5.53	53.22±2.76
K_{TH}	0.0645±0.0083	0.0719±0.0088	0.0867±0.0098
T	0.823±0.165	0.882±0.219	0.531±0.150
R^2	0.987	0.987	0.977
SS	1.39	2.47	4.78

3.7. Thermodynamic parameters of adsorption

To estimate the effect of temperature on the adsorption of CR on CCIO, the free Gibbs energy change (ΔG^0), enthalpy change (ΔH^0), and entropy change (ΔS^0) were determined. The apparent equilibrium constant (K_c') of the biosorption was defined as:

$$K_c' = c_{ad,e} / c_e \quad (9)$$

where $c_{ad,e}$ is the concentration of CR on the adsorbent at equilibrium (mg l^{-1}) [39]. The value of K_c' in the lowest experimental CR concentration can be obtained. The K_c' value is used in the following equation to determine the Gibbs free energy of biosorption (ΔG^0).

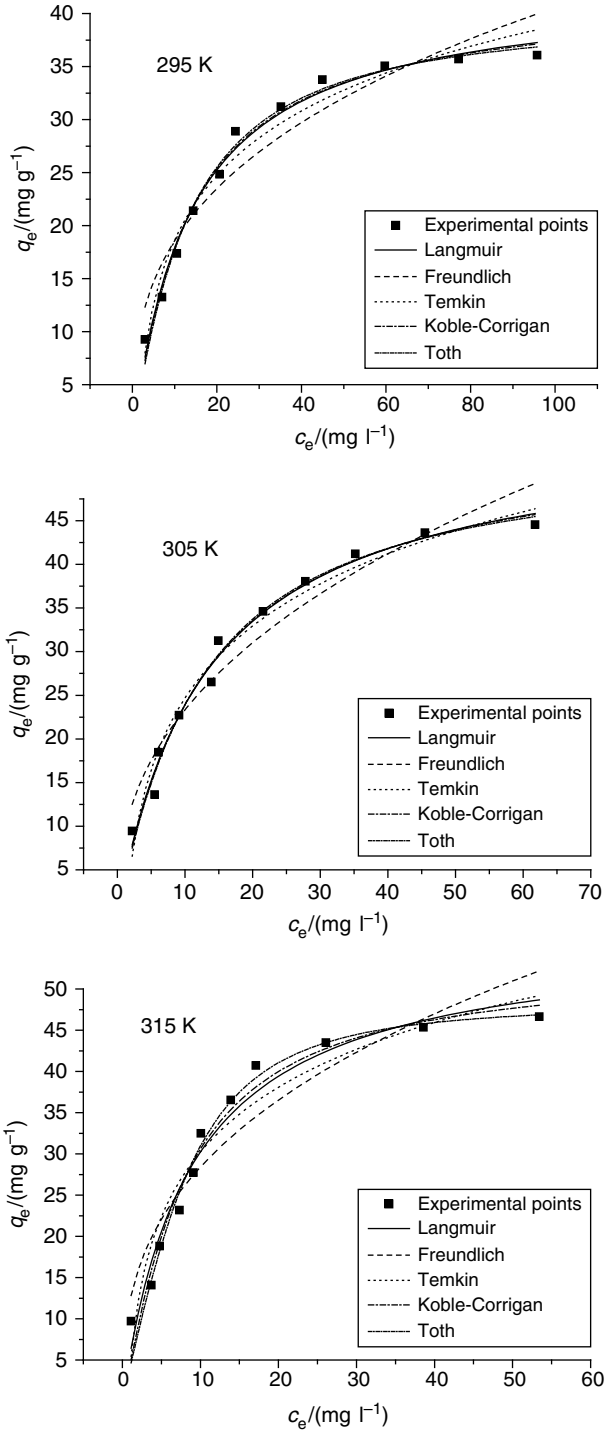

Fig. 6. Comparison of experimental adsorption isotherms and fitted isotherms by different models.

$$\Delta G^0 = -RT\ln K_c' \quad (10)$$

The enthalpy (ΔH^0) and entropy (ΔS^0) can be obtained from the slope and intercept of the van't Hoff plot of ΔG^0 versus T:

$$\Delta G^0 = \Delta H^0 - T\Delta S^0 \quad (11)$$

where ΔG^0 is Gibbs free energy change, J; R is universal gas constant, 8.314 J mol^{-1} K^{-1} and T is absolute temperature, K.

Values of ΔG^0, ΔH^0, ΔS^0 for the adsorption process obtained from Eq. (9) and (10) are listed in Table 2.

The negative ΔG^0 values of CR at various temperatures in Table 2 were due to the fact that the adsorption processes were spontaneous with a high preference of CR on CCIO. The negative value of ΔG^0 decreased with an increase in temperature. This indicated that the spontaneous nature of adsorption of CR was proportional to the temperature and higher temperature was favor of adsorption process [39].

Basically, the heat evolved during physical adsorption falls into a range of 2.1–20.9 kJ mol^{-1}, while the heat of chemisorption generally falls into a range of 80–200 kJ mol^{-1} [32]. But the value of ΔH^0 in Table 2 was 39.96 kJ mol^{-1}. Therefore, it seemed that CR adsorption by CCIO would be attributed to a physico-chemical adsorption process rather than a pure physical or chemical adsorption process.

The positive value of ΔH^0 confirmed the endothermic character of adsorption in nuture. The positive value of ΔS^0 suggested the increased randomness at the solid–solution interface during the adsorption process and the affinity of CCIO toward CR ions in aqueous solutions. The adsorbed solvent molecules which are displaced by the adsorbate species gain more translational entropy than ions lost by adsorbate thus allowing for prevalence of randomness in the system [40].

3.8. Regeneration of CR-loaded CCIO

Investigation on the desorption of the dye from the adsorbent is necessary for its reuse and also to understand the mechanism of adsorption. It may decrease the process cost and also the dependency of the process on a continuous adsorbent supply [19,20]. For this purpose, it is desirable to desorb the adsorbed dyes and to regenerate the adsorbent for another cycle of application. Also desorption studies help elucidate the mechanism of adsorption. If only water was used to regenerate spent

Table 2
Thermodynamic parameters of CR adsorption

Thermodynamic parameters	Temperature/K		
	295	305	315
ΔG^0 (kJ mol^{-1})	−6.17	−7.22	−9.28
ΔH^0 (kJ mol^{-1})		39.96	
ΔS^0 (kJ mol^{-1} K^{-1})		0.156	

adsorbent, the removal efficiency of CR was only 30% in second use. But when dilute NaOH solution (0.01 mol l^{-1}) was used, the removal efficiency of CR is 90%, 80%, 75%, respectively when CCIO was used in first, second and third cycles. Only the physisorbed CR unlike the chemisorbed species might be desorbed from the adsorbent surface by water. This result showed that the chemisorption might be the major mode of adsorption [41]. Complete regeneration of dye-loaded CCIO was not possible under alkali treatment, suggesting chemisorption of dye molecules on CCIO.

3.9. Mechanism of adsorption

The FT-IR analysis (figure not shown) showed that the peaks were mainly from contribution of –OH and –NH stretching (3360 cm^{-1}), C–H stretching (2905 cm^{-1}), 1638 cm^{-1} (–NH bending in $–NH_2$), 1065 cm^{-1} (–C–O–C– stretching), Fe–O bond vibration of Fe_3O_4 (560–660 cm^{-1}). This revealed that the functional groups such as $–NH_2$, –OH, originally presented in chitosan, were intact after coating on Fe_3O_4 and were available for interaction with the dye.

Chitosan has potential as an adsorbent for removal of CR from textile wastewater because it efficiently adsorbed dyes over a wide pH range. Under acidic conditions, the amine groups ($–NH_2$) of chitosan is protonated as $–NH_3^+$. In aqueous solutions, the synthetic reactive dye, including CR, is dissolved and the sulfonate group of the reactive dye is dissociated and converted to anionic dye ions:

$$DSO_3Na \xrightarrow{H_2O} DSO_3^- + Na^+$$

The adsorption process then proceeds due to the electrostatic interaction between these two counter ions and forms an ion pair (protonated group and anion) [28,42]. As a result, these ion pairs can act as anion adsorption sites [37]:

$$R' – NH_3^+ + DSO_3^- \rightleftharpoons R' – NH_3^{+-}O_3SD$$

This result demonstrated an ion exchange mechanism.

But at pH over 7, surface charge of chitosan beads is negative which hinders the adsorption by electrostatic force of repulsion between the negatively charged dye molecule and adsorbent. But the values of q_e did not significantly decrease (see Fig. 1). There is every possibility of hydrogen bond formation between some of the molecular components of congo red such as N, S, O, benzene ring and CH_2OH groups of the chitosan molecule. This fact suggests strong involvement of other interactions as hydrogen bonds, van der Waals force, etc. in the adsorption process as there are hydroxyl groups in chitosan and amine group in CR [37,43]. Sakkayawong et al. reported that the mechanism under acidic conditions was chemical adsorption for reactive dye adsorption on chitosan, while under caustic conditions the mechanism was both physical and chemical adsorption [28].

4. Conclusion

CR adsorption from aqueous solution using CCIO was investigated under different experimental conditions in batch mode. The values of q_e for CR adsorption were dependent on contact time, temperature and dye concentration. The solution pH and salt concentration had little effect on CR adsorption. The equilibrium data were found to be better represented by the Langmuir, Toth and the Koble–Corrigan isotherms according to the nonlinear regressive analysis. The adsorption process was spontaneous and endothermic. The process was main chemical adsorption. The dye-loaded adsorbent was regenerated by dilute NaOH solution. The CCIO can be used to remove anionic dye from solution.

Acknowledgment

This work was supported by the National Natural Science Foundation of China for undergraduate cultivation in basic science (J0830412), the Natural Science Foundation of Henan Province (No 92300410030).

Appendix

The structure of CR is following:

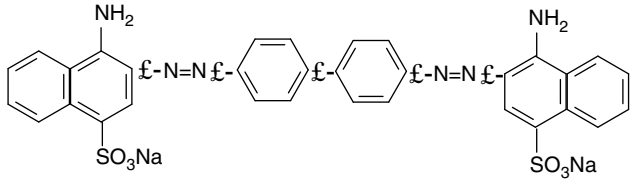

References

[1] G. Crini and P.M. Badot, Application of chitosan, a natural aminopolysaccharide, for dye removal from aqueous solutions by adsorption processes using batch studies: A review of recent literature, Prog. Polym. Sci., 33 (2008) 399–447.
[2] M. Rinaudo, Chitin and chitosan: Properties and applications, Prog. Polym. Sci., 31 (2006) 603–632.
[3] E. Guibal, Interactions of metal ions with chitosan-based sorbents: a review, Sep. Purif. Technol., 38 (2004) 43–74.
[4] F.C. Wu, R.L. Tseng and R.S. Juang, A review and experimental verification of using chitosan and its derivatives as adsorbents for selected heavy metals, J. Environ. Manage., 91 (2010) 798–806.

[5] V.M. Boddu, K. Abburi, J.L. Talbott and E.D. Smith, Removal of hexavalent chromium from wastewater using a new composite chitosan biosorbent, Environ. Sci. Technol., 37 (2003) 4449–4456.
[6] V.M. Boddu, K. Abburi, J.L. Talbott, E.D. Smith and R. Haasch, Removal of arsenic (III) and arsenic(V) from aqueous medium using chitosan-coated biosorbent, Water Res., 42 (2008) 633–642.
[7] S. Hasan, T.K. Ghosha, D.S. Viswanath and V.M. Boddu, Dispersion of chitosan on perlite for enhancement of copper(II) adsorption capacity, J. Hazard. Mater., 152 (2008) 826–837.
[8] S.R. Popuri, Y. Vijaya, V.M. Boddu and K. Abburi, Adsorptive removal of copper and nickel ions from water using chitosan coated PVC beads, Bioresour. Technol., 100 (2009) 194–199.
[9] M.W. Wan, I.G. Petrisor, H.T. Lai, D. Kim and T.F. Yen, Copper adsorption through chitosan immobilized on sand to demonstrate the feasibility for in situ soil decontamination, Carbohydr. Polym., 55 (2004) 249–254.
[10] B.T. Liu, R.T. Li and A.X. Jiang, Equilibrium studies for reactive dye absorption onto chitosan supported by bentonite, J. Nat. Sci..Heilongjiang Uni., 23 (2006) 45–48 (in Chinese).
[11] M.Y. Chang and R.S. Juang, Adsorption of tannic acid, humic acid, and dyes from water using the composite of chitosan and activated clay, J. Colloid Interface. Sci., 278 (2004) 18–25.
[12] T. Robinson, G. McMullan, R. Marchant and P. Nigam, Remediation of dyes in textile effluent: a critical review on current treatment technologies with a proposed alternative, Bioresour. Technol., 77 (2001) 247–255.
[13] G. Crini, Non-conventional low-cost adsorbents for dye removal: A review, Bioresour. Technol., 97 (2006) 1061–1085.
[14] V.K. Gupta and Suhas, Application of low cost adsorbents for dye removal- A review, J. Environ. Manage., 90 (2009) 2313–2342.
[15] R.P. Han, Y.F. Wang, P. Han, J. Shi, J. Yang and Y.S. Lu, Removal of methylene blue from aqueous solution by chaff in batch mode, J. Hazard. Mater., 137 (2006) 550–557.
[16] R.P. Han, D.D. Ding, Y.F. Xu, W.H. Zou, Y.F. Wang, Y.F. Li and L.N. Zou, Use of rice husk for the adsorption of congo red from aqueous solution in column mode, Bioresour. Technol., 99 (2008) 2938–2946.
[17] A. Mittal, J. Mittal, A. Malviya, D. Kaur, V.K. Gupta, Adsorption of hazardous dye crystal violet from wastewater by waste materials, J. Colloid Interface Sci., 343 (2010) 463–473.
[18] J.X. Lin and L. Wang, Adsorption of dyes using magnesium hydroxide-modified diatomite, Desalin. Water Treat., 8 (2009) 263–271.
[19] R.P. Han, Y. Wang, Q. Sun, L.L. Wang, J.Y. Song, X.T. He and C.C. Dou, Malachite green adsorption onto natural zeolite and reuse by microwave irradiation, J. Hazard Mater., 175 (2010) 1056–1061.
[20] R.P. Han, L.N. Zou, X. Zhao, Y.F. Xu, Y.F. Li, Y.L. Li and Y. Wang, Characterization and properties of iron oxide-coated zeolite as adsorbent for removal of copper (II) from solution in fixed bed column, Chem. Eng. J., 149 (2009) 123–131.
[21] S.B. Wang and E. Ariyanto, Competitive adsorption of malachite green and Pb ions on natural zeolite, J. Colloid Interface Sci., 314 (2007) 25–31.
[22] L. Zhao, W.H. Zou, L.N. Zou, X.T. He, J.Y. Song and R.P. Han, Adsorption of methylene blue and methyl orange from aqueous solution by iron oxide-coated zeolite in fixed bed column: predicted curves, Desalin. Water Treat., 22 (2010) 258–264.
[23] V.K. Gupta and I. Ali, Removal of endosulfan and methoxychlor from water on carbon slurry, Environ. Sci. Technol., 42 (2008) 766–770.
[24] X.L. Wu, Y. Wang, J.L. Liu, J.Y. Ma and R.P. Han, Study of Malachite Green adsorption onto natural zeolite in fixed-bed column, Desalin. Water Treat., 20 (2010) 228–233.
[25] S.B. Wang, T. Terdkiatburana and M.O. Tadé, Single and co-adsorption of heavy metals and humic acid on fly ash, Sep. Purif. Technol., 58 (2008) 353–358.
[26] R. Srivastava and D.C. Rupainwar, Liquid phase adsorption of indigo carmine and methylene blue on neem bark, Desalin. Water Treat., 24 (2010) 74–84.
[27] Y.J. Wu, L.J. Zhang, C.L. Gao, J.Y. Ma, X.H. Ma and R.P. Han, Adsorption of copper ions and methylene blue in single and binary system on wheat straw, J. Chem. Eng. Data, 54 (2009) 3229–3234.
[28] I. Langmuir, The constitution and fundamental properties of solids and liquids, J. Am. Chem. Soc., 38 (1916) 2221–2295.
[29] H.M.F. Freundlich, Uber die adsorption in lasungen, Z. Phys. Chem., 57 (1906) 385–470.
[30] X.C. Fu, W.X. Shen and T.Y. Yao, Physical Chemistry (Fourth edition), Higher Education Press, China (1994) 303–321.
[31] R.A. Koble and T.E. Corrigan, Adsorption isotherms for pure hydrocarbons, Ind. Eng. Chem., 44 (1952) 383–387.
[32] Y. Liu and Y.J. Liu, Biosorption isotherms, kinetics and thermodynamics, Sep. Purif. Technol., 61 (2008) 229–242.
[33] N. Sakkayawong, P. Thiravetyan and W. Nakbanpote, Adsorption mechanism of synthetic reactive dye wastewater by chitosan, J. Colloid Interface Sci., 286 (2005) 36–42.
[34] L. Wang and A.Q. Wang, Adsorption characteristics of Congo Red onto the chitosan/montmorillonite nanocomposite, J. Hazard. Mater., 147 (2007) 979–985.
[35] W.H. Zou, P. Han, Y.L. Li, X. Liu, X.T. He and R.P. Han, Equilibrium, kinetic and mechanism study for the adsorption of neutral red onto rice husk, Desalin. Water Treat., 12 (2009) 210–218.
[36] Y.S. Al-Degs, M.I. El-Barghouthi, A.H. El-Sheikh and G.M. Walker, Effect of solution pH, ionic strength, and temperature on adsorption behavior of reactive dyes on activated carbon, Dyes Pigments, 77 (2008) 16–23.
[37] N.S. Maurya, A.K. Mittal, P. Cornel and E. Rother, Biosorption of dyes using dead macro fungi: Effect of dye structure, ionic strength and pH, Bioresour. Technol., 97 (2006) 512–521.
[38] S. Chatterjee, S. Chatterjee., B.P. Chatterjee and A.K. Guha, Adsorptive removal of congo red, a carcinogenic textile dye by chitosan hydrobeads: Binding mechanism, equilibrium and kinetics, Colloids Surf. A., 299 (2007) 146–152.
[39] Z. Aksu, Determination of the equilibrium, kinetic and thermodynamic parameters of the batch biosorption of nickel(II) ions onto *Chlorella vulgaris*, Process Biochem., 38 (2002) 89–99.
[40] M.M. Abd El- Latif and Amal M. Ibrahim, Adsorption, kinetic and equilibrium studies on removal of basic dye from aqueous solutions using hydrolyzed Oak sawdust, Desalin. Water Treat., 6 (2009) 252–268.
[41] C. Namasivayam and D. Kavitha, Removal of Congo Red from water by adsorption onto activated carbon prepared from coir pith, an agricultural solid waste, Dyes Pigments, 54 (2002) 47–58.
[42] Y.C. Wong, Y.S. Szeto, W.H. Cheung and G. McKay, Adsorption of acid dyes on chitosan equilibrium isotherm analyses, Process Biochem., 39 (2004) 693–702.
[43] J.H. An and S. Dultz, Adsorption of tannic acid on chitosan-montmorillonite as a function of pH and surface charge properties, Appl. Clay Sci., 36 (2007) 256–264.